Stem Cell Research (2012) 9, 225–236

Available online at www.sciencedirect.com

SciVerse ScienceDirect

www.elsevier.com/locate/scr

REGULAR ARTICLE

Impact of hypoxia and long-term cultivation on the genomic stability and mitochondrial performance of *ex vivo* expanded human stem/stromal cells

Pedro H. Oliveira [a], Joana S. Boura [a], Manuel M. Abecasis [b], Jeffrey M. Gimble [c], Cláudia Lobato da Silva [a], Joaquim M.S. Cabral [a,*]

[a] *Department of Bioengineering and Institute for Biotechnology and Bioengineering, Instituto Superior Técnico (IST), Technical University of Lisbon, Lisboa, Portugal*
[b] *IPOFG-Instituto Português de Oncologia Francisco Gentil, Lisboa, Portugal*
[c] *Pennington Biomedical Research Center, Louisiana State University System, Baton Rouge, LA, USA*

Received 13 February 2012; received in revised form 10 July 2012; accepted 13 July 2012
Available online 23 July 2012

Abstract Recent studies have described the occurrence of chromosomal abnormalities and mitochondrial dysfunction in human stem/stromal cells (SCs), particularly after extensive passaging *in vitro* and/or expansion under low oxygen tensions. To deepen this knowledge we investigated the influence of hypoxia (2% O_2) and prolonged passaging (>P10) of human bone marrow stromal cells (BMSCs) and adipose-derived stromal cells (ASCs) on the expression of genes involved in DNA repair and cell-cycle regulation pathways, as well as on the occurrence of microsatellite instability and changes in telomere length. Our results show that hypoxic conditions induce an immediate and concerted down-regulation of genes involved in DNA repair and damage response pathways (*MLH1*, *RAD51*, *BRCA1*, and *Ku80*), concomitantly with the occurrence of microsatellite instability while maintaining telomere length. We further searched for mutations occurring in the mitochondrial genome, and monitored changes in intracellular ATP content, membrane potential and mitochondrial DNA content. Hypoxia led to a simultaneous decrease in ATP content and in the number of mitochondrial genomes, whereas the opposite effect was observed after prolonged passaging. Moreover, we show that neither hypoxia nor prolonged passaging significantly affected the integrity of the mitochondrial genome. Ultimately, we present evidence on how hypoxia selectively impacts the cellular response of BMSCs and ASCs, thus pointing for the need to optimize oxygen tension according to the cell source.

Introduction

Stem/stromal cells (SCs) consist of a population of non-hematopoietic multipotent progenitors, able to differentiate into different mesodermal cell lineages, and which can be isolated from adult tissues (*e.g.* bone marrow (BM), the most studied source) or postnatal tissues (*e.g.* umbilical cord matrix). An increasing body of evidence has demonstrated the immense clinical potential of SCs, mainly resulting from their immunomodulatory properties and multilineage differentiation ability. Some examples of the latter include the

* Corresponding author. Fax: +351 218419062.
E-mail address: joaquim.cabral@ist.utl.pt (J.M.S. Cabral).

1873-5061/$ - see front matter © 2012 Elsevier B.V. All rights reserved.
http://dx.doi.org/10.1016/j.scr.2012.07.001

treatment of myocardial infarction (Strauer et al., 2002; Chen et al., 2004), *osteogenesis imperfecta* (Horwitz et al., 2001), and in the context of hematopoietic cell transplantation, improving hematopoietic engraftment and preventing or attenuating the effects of graft-*versus*-host-disease (Lazarus et al., 2005).

Since BMSC titers are typically very low and decline with age (roughly 0.01% of BM mononuclear cells in a newborn in

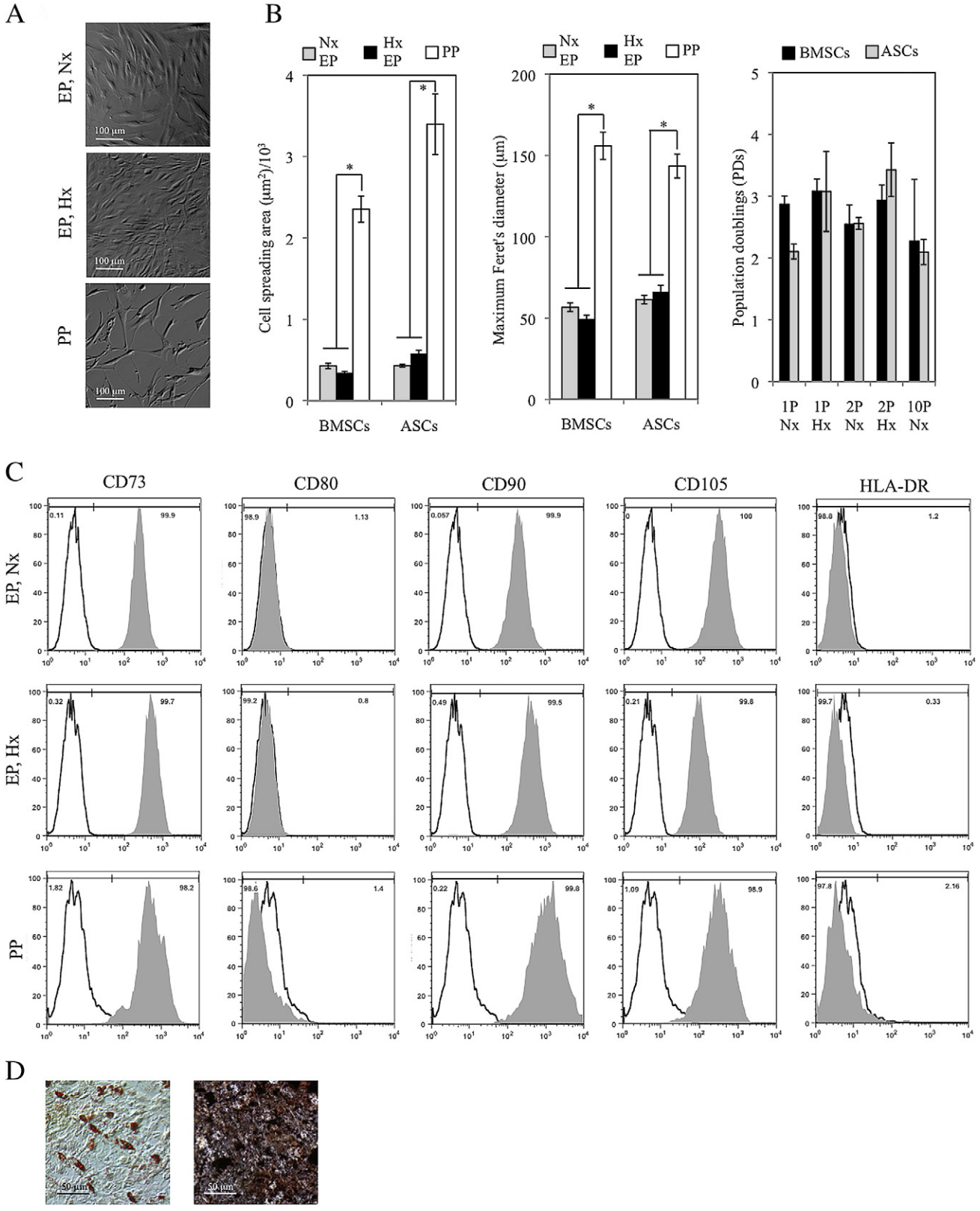

opposition to 0.00005% in elderly patients) (Caplan, 2007), it becomes necessary to expand these cells *ex vivo* in order to achieve clinically relevant cell numbers. Concurrently, other sources such as the adipose tissue are emerging as an alternative source of SCs, which can thus be obtained in a less invasive way, and in larger titers than those found in the BM (Gimble and Guilak, 2003).

The process of expanding adult stem cells *in vitro*, namely SCs, has proven to be challenging not only from the bioengineering standpoint (Dos Santos et al., 2010; Eibes et al., 2010; Santos et al., 2011), but also from the perspective of maintaining stem cell characteristics while avoiding or delaying senescence and genetic instability (Tarte et al., 2010; Sensebe et al., 2011; Ueyama et al., 2012). In this sense, several studies have pointed out that the *ex vivo* propagation of adult stem cells, particularly for extended periods of time, induces a cascade of cellular events that lead to a decay in proliferation rate and differentiation potential (Bonab et al., 2006), compromised mitochondrial function (Rubio et al., 2008), and increased number of chromosomal abnormalities (Izadpanah et al., 2008; Tarte et al., 2010). Moreover, the use of low oxygen tensions (1–5%, referred to as hypoxia) has been exploited as a strategy to mimic the physiologic microenvironment of these cells in order to increase cell proliferation (Dos Santos et al., 2010; Tsai et al., 2011). Nevertheless, the mechanisms involved are poorly understood and some conflicting results have been obtained. One example of the latter includes determining to what extent hypoxic environments affect the expression of certain cell-cycle-related or DNA repair genes, therefore disturbing genetic stability (Bindra et al., 2007; Rodriguez-Jimenez et al., 2008; Yeung et al., 2008). The role of hypoxia as modulator of several functional mitochondrial properties in adult stem cells, namely its metabolic activity or the presence of deleterious mutations, also remains to be clarified (Rehman, 2010).

In this work, we present a side-by-side comparison of human BMSCs and ASCs concerning the impact of prolonged passaging (>P10, PP) and use of a low oxygen tension (2%) on the expression of the proto-oncogene *c-MYC* and tumor suppressor gene *p53*, as well as on critical genes that mediate mismatch repair (MMR), homologous recombination (HR) and non-homologous end-joining (NHEJ). We further examined the influence of the aforementioned conditions in the onset of microsatellite instability (MSI), changes in telomere length, and mitochondrial performance. In addition, to gain insight into so far unnoticed discrepancies between BMSCs and ASCs responses to hypoxia, our results provide data potentially useful in the specification of quality-control requirements for stem-cell-based products for use in Cellular Therapy applications. Moreover, they extend the current knowledge on the continuous and far reaching changes occurring at the cellular level, that need to be taken into account when considering the *ex vivo* expansion of SCs for therapeutic applications.

Materials and methods

Human bone marrow and adipose-derived stem/stromal cell cultures

Human bone marrow aspirates were obtained from healthy donors (n=3, ages between 42 and 47 years old, P1–P5) after informed consent, at Instituto Português de Oncologia Francisco Gentil, Lisboa, Portugal. BMSCs were isolated and characterized according to the protocol described by Dos Santos et al. (2010). ASCs were obtained from adult human subcutaneous adipose tissue (n=4, ages between 25 and 59 years old, P1–P5), as described previously (Gimble and Guilak, 2003). Both cell types were cultured in Dulbecco's Modified Essential Medium, DMEM (Gibco, Grand Island, NY) supplemented with 10% qualified fetal bovine serum, FBS (Gibco) and 1% penicillin–streptomycin–fungizone (Gibco) at 37 °C and 5% CO_2 in a humidified atmosphere. Hypoxia cultivation of BMSCs and ASCs was established in a Napco 8000WJ incubator (Thermo Scientific, Waltham, MA) flushed with premixed 2% O_2 and 5% CO_2 at 37 °C. Exhausted medium was changed twice a week and cell passaging was performed near confluence (>80%) under normoxia. Briefly, cells were washed with phosphate buffered saline (PBS) (Gibco) and detached from the T-flask by adding Accutase solution (Sigma, St. Louis, MO) for 7 min at 37 °C. Cell number and viability were determined using the Trypan Blue (Gibco) exclusion method. Replating was performed at an initial density of 5000 cells/cm^2. The number of population doublings (PDs) was calculated according to $PDs = \log[(\textit{number of harvested cells})/(\textit{number of plated cells})]/\log(2)$.

Cell morphological analysis

Analysis of cell morphology was routinely performed using bright field microscopy (Olympus, Hamburg, Germany). Image analysis in terms of cell surface area (spreading) and Feret's diameter was conducted using the NIH ImageJ software v. 1.44 (http://rsbweb.nih.gov/ij/) after outlining cell boundaries.

Figure 1 Morphology, analysis of surface markers and differentiation potential of SCs. Representative images of BMSCs exhibiting a fibroblastic morphology in early passages (EP, P1–P5) in both normoxia and hypoxia (A, EP Nx, EP Hx), or showing an enlarged and irregular shape typical of a pre-senescent/senescent state after prolonged passaging (>P10) in normoxia (A, PP). Similar changes in morphology were observed in ASCs (Supplementary Fig. 1A). The ImageJ software was used to compute cell spreading area and maximum Feret's diameter (B). The morphology of BMSCs and ASCs expanded under normoxia (Nx, gray bars) or 2% hypoxia (Hx, black bars) at early passages was compared with prolonged passage cells under normoxia (white bars). *$p<0.05$. Also, the number of population doublings (PDs) did not change significantly between BMSCs and ADSc expanded under normoxia or hypoxia for 14 days, or alternatively under normoxia for ten consecutive passages (B). (C) Representative analysis of BMSC surface markers for EP Nx, EP Hx and PP. Similar results were observed with ASCs (Supplementary Fig. 1C). (D) Representative images of the *in vitro* differentiation of BMSCs along adipogenic (left) and osteogenic (right) lineages. After adipogenic differentiation, Oil Red O staining revealed the presence of lipid vesicles (in red) (left). After osteogenic differentiation, alkaline phosphatase was used to stain osteogenic progenitors (shown in pink) while von Kossa staining revealed the presence of calcium deposits (shown in black) (right). Similar results were observed with ASCs (Supplementary Fig. 1B).

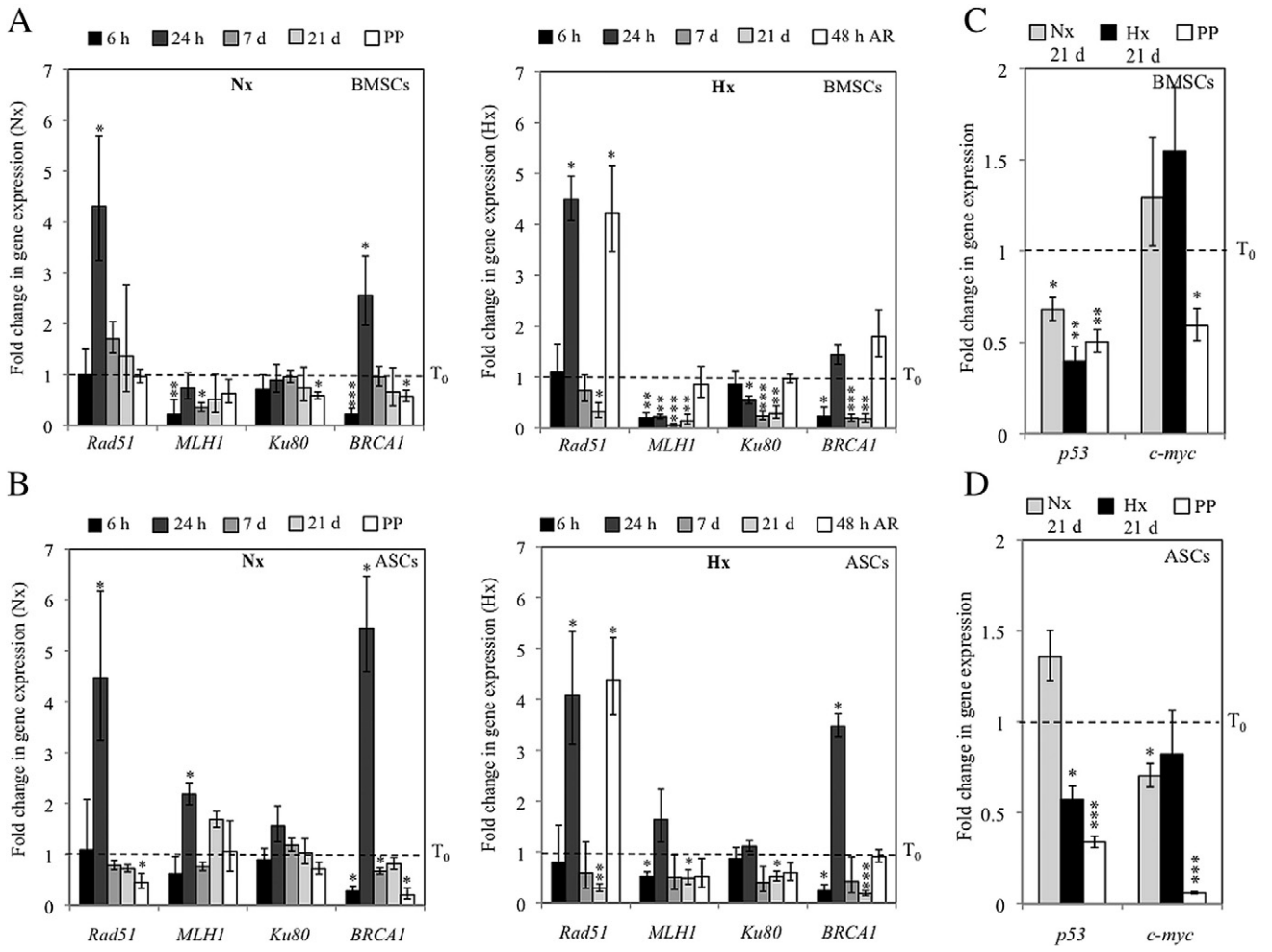

Figure 2 Changes in the expression level of DNA repair genes, tumor suppressor *p53*, and *c-MYC* proto-oncogene in BMSCs and ASCs expanded for different incubation times under normoxia (Nx), 2% hypoxia (Hx) and 48 h after reoxygenation (AR). (A, B) Fold change in the expression of HR (*RAD51*, *BRCA1*), NHEJ (*Ku80*), and MMR (*MLH1*) genes, normalized to T_0. (C, D) Fold change in the expression of *p53* and *c-MYC*, normalized to T_0. *GAPDH* was used as housekeeping gene (results using *ACTB* are shown in Supplementary Fig. 2A). Results are shown for both cell sources expanded for 21 days under Nx and Hx or for PP in Nx. $^*p<0.05$, $^{**}p<0.01$, $^{***}p<0.001$.

The latter parameter is the maximum measured distance between parallel lines tangent to the cell boundaries and perpendicular to the ocular scale. At least three fields of view per condition and per donor were used (n=20), and each measurement was performed in triplicate.

Immunophenotyping and *in vitro* multilineage differentiation

Immunophenotyping was performed according to (Santos et al., 2011). Briefly, a panel of PE-conjugated mouse anti-human monoclonal antibodies was used: CD73 (Becton Dickinson Immunocytometry Systems, San Jose, CA), CD80 (BioLegend, San Diego, CA), CD90 (R&D Systems, Minneapolis, MN), CD105 (Invitrogen, Carlsbad, CA), and human leukocyte antigen (HLA)-DR (Becton Dickinson Immunocytometry Systems). Appropriate isotype controls were used in every experiment and a minimum of 10,000 events was collected for each sample. Cells were analyzed in a FACSCalibur (Becton Dickinson Biosciences) using the CellQuest software (Becton Dickinson Biosciences).

For *in vitro* multilineage differentiation, SC cultures were allowed to reach confluence, and were subsequently induced to differentiate towards the adipogenic and osteogenic lineages by replacing the expansion medium with those provided in the STEMPRO® Adipogenesis and Osteogenic Differentiation medium (Gibco) respectively. Cultures were re-fed every 3 days for a period of two weeks, after which their differentiation potential was evaluated. For this purpose, cells were washed with PBS, fixed with 2% (w/v) paraformaldehyde (PFA) (Sigma) for 30 min, and washed again with deionized water (dH_2O). The extent of adipogenic differentiation was assessed by Oil Red O staining (Sigma) (0.3% in isopropanol) for 1 h at room temperature, after which cells were washed with dH_2O and visualized under the microscope. Osteogenic differentiation was evaluated by staining for alkaline phosphatase using Naphtol AS-MX phosphate and Fast Violet (both from Sigma) for 45 min at room temperature, washing three times with dH_2O, and visualizing under the microscope. For von Kossa staining, cells were incubated with silver nitrate (2.5% w/v) (Sigma) for 30 min, washed three times with dH_2O, and visualized under the microscope.

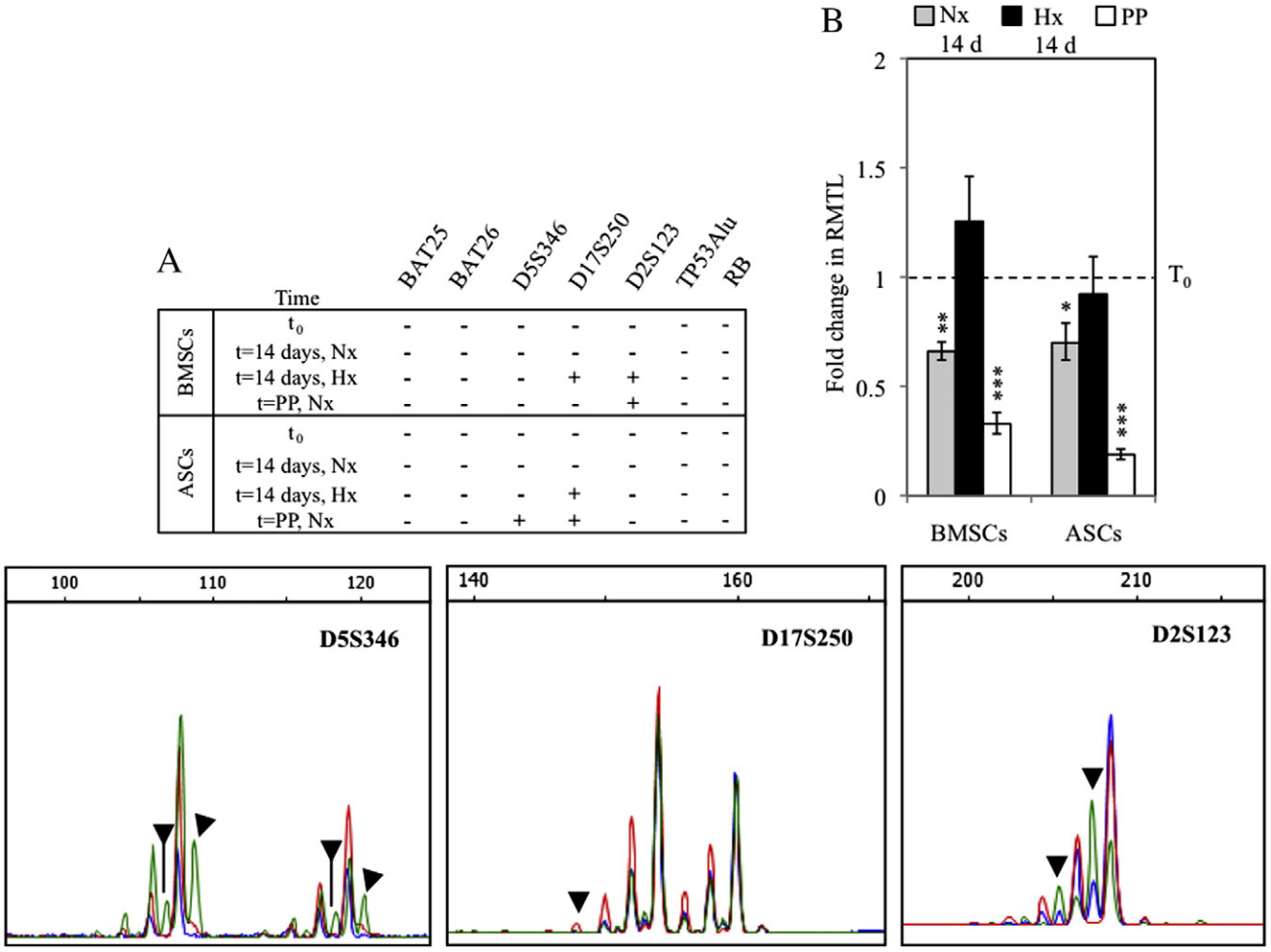

Figure 3 Impact of hypoxia and PP on the onset of microsatellite instability (MSI) and on relative mean telomere length (RMTL). (A) The occurrence of MSI was evaluated in the Bethesda panel of markers (BAT25, BAT26, D5S346, D17S250, and D2S123) as well as in TP53Alu and RB. Minus (−) or plus (+) signs respectively denote MSI negative and MSI positive samples. The result was scored as positive when at least one donor revealed MSI. Overall, samples were found to be stable (MSI-S) if no unstable locus was found or low-frequency (MSI-L) for those in which less than 40% of the loci were unstable. Representative electropherograms depicting unstable *loci* are also shown (t_0 — blue; Hx 21 days — red; PP — green), with additional or missing peaks indicated by arrows. (B) Fold-change in RMTL using *GAPDH* as comparison (results using *ACTB* are shown in Supplementary Fig. 2B). $^{*}p<0.05$, $^{**}p<0.01$, $^{***}p<0.001$.

Gene expression analysis by real-time polymerase chain reaction (RT-PCR)

Total RNA from BMSCs and ASCs was extracted using the High Pure RNA isolation kit (Roche Diagnostics, Mannheim, Germany) following the manufacturer's instructions. Total RNA samples (1 μg) were independently reverse-transcribed by oligo(dT) priming using the Transcriptor First-Strand cDNA synthesis kit (Roche). All RT-PCR reactions were carried out in a Roche Light Cycler™ detection system and in a 20 μl final volume containing 2.0 mM $MgCl_2$ solution, 0.2 μM of each primer, 2.0 μl of sample and SYBR Green I mixture. The amplification program was as follows: 10 min at 95 °C followed by 40 cycles of 10 s at 95 °C, 5 s at 55 °C and 10 s at 72 °C. Reactions were finally kept at 70 °C for 30 s and heat-denatured over a temperature gradient of 0.1 °C/s from 70 to 95 °C. The comparative threshold cycle (C_T) method was used to calculate the expression of *MLH1*, *RAD51*, *BRCA1*, *Ku80*, *p53* and *c-MYC* relative to two endogenous reference genes (*GAPDH* and *ACTB*) (primer sequences are listed in Supplementary Table 1). While some studies have provided evidence for hypoxic-mediated changes in *GAPDH* gene expression, others do not show such relation (Said et al., 2007; Rodriguez-Jimenez et al., 2008; Basciano et al., 2011). We verified that under our experimental conditions the expression of both genes did not significantly change ($p>0.05$) with varying oxygen tension nor prolonged passaging. The ΔC_T parameter was calculated for both normoxic and hypoxic samples as $\Delta C_T = C_T$ (*gene of interest*) $- C_T$ (*housekeeping gene*). The fold variation in gene expression was finally given by $2^{-\Delta\Delta C_T}$ where $\Delta\Delta C_T = \Delta C_T$ (time t) $- \Delta C_T$ (time 0).

Microsatellite instability (MSI) analysis

Genomic DNA was extracted from BMSCs and ASCs by using the Wizard Genomic DNA purification kit (Promega, Madison, WI),

and quantified spectrophotometrically. For the determination of microsatellite instability (MSI), we evaluated TP53Alu, RB, and the Bethesda panel of five microsatellite markers recommended by the National Cancer Institute: two mononucleotide repeats (BAT25, BAT26) and three dinucleotide repeats (D5S346, D2S123, and D17S250). All forward primers were fluorescein-labeled with [6-FAM] (Supplementary Table 1). PCR reactions were carried out in a 20 μl mixture containing 100 ng gDNA, 0.5 μM of each primer, 2.5 mM $MgCl_2$, 500 μM each DNTP and 0.5 U of AmpliTaq Gold DNA polymerase (Applied Biosystems, Foster City, CA). PCR was carried out in a Biometra T Gradient thermal cycler (Goettingen, Germany) according to the following program: 10 min at 94 °C followed by 40 cycles of 45 s at 94 °C, 45 s at T_a °C, 45 s at 72 °C, and a final extension step of 10 min at 72 °C. The values for T_a were based on (Dietmaier et al., 1997), and were 52 °C (D17S250), 55 °C (D5S346), 58 °C (BAT25, BAT26, TP53Alu, and RB), or 60 °C (D2S123). Finally, PCR products were 10–20-fold diluted in water, and 1.5 μl of the latter was mixed with 18 μl of deionized formamide (Applied Biosystems) and 0.5 μl GeneScan ROX 350 size standard (Applied Biosystems). MSI status was categorized according to the following criteria: stable (MSI-S) if none of the loci revealed MSI, low-frequency (MSI-L) if less than 40% of the loci were unstable, high-frequency (MSI-H) if more than 40% of the loci were unstable (Dietmaier et al., 1997). To exclude potential artifacts inherent to the PCR process, MSI status was only scored when changes could be reproduced in at least two independent PCR reactions.

Telomere length analysis

Relative mean telomere length (RMTL) was assessed by real time PCR using a modified version of the assay initially described elsewhere (Cawthon, 2002). Briefly, the telomere

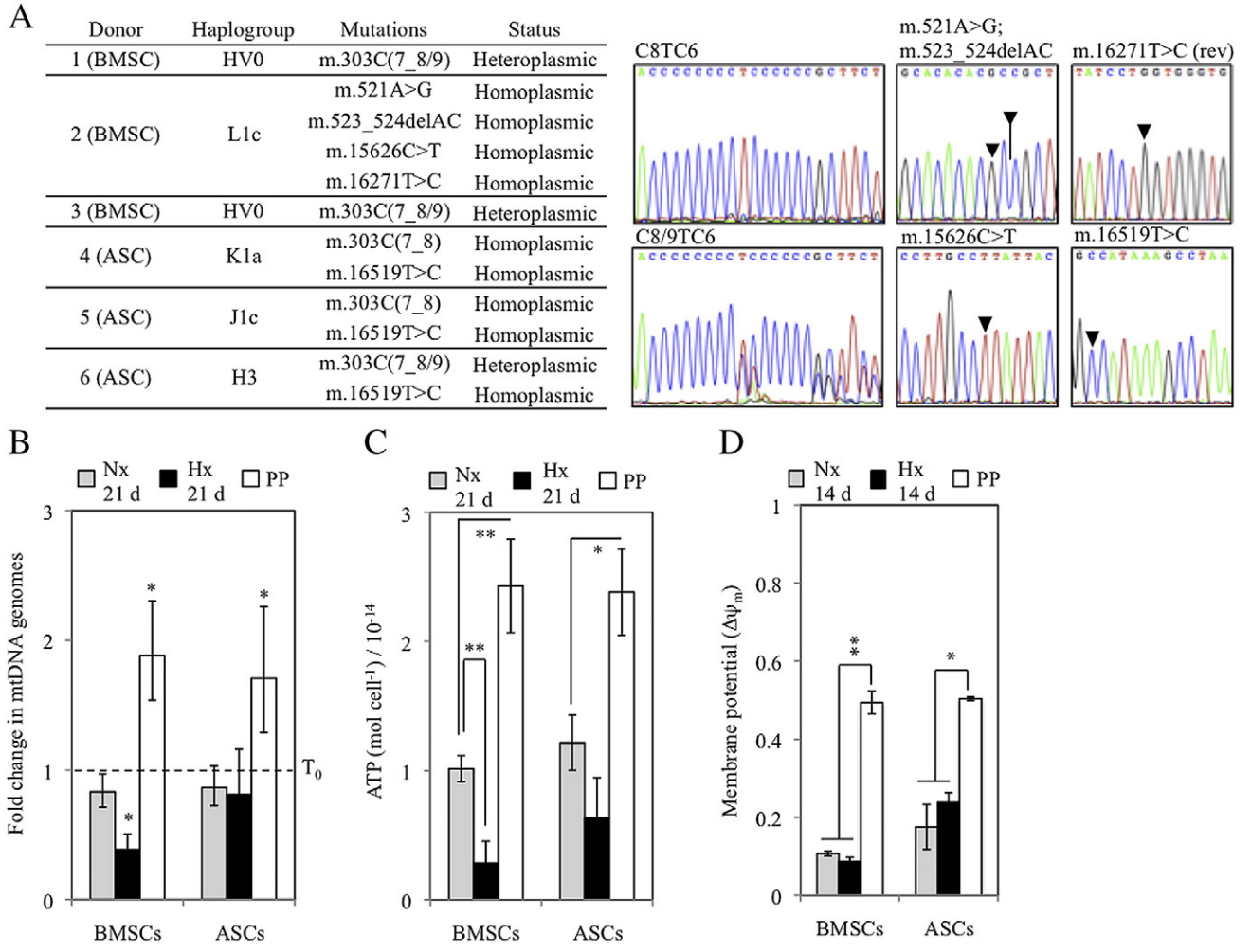

Figure 4 Evaluation of mitochondrial properties in SCs. (A) Sequencing of the complete mitochondrial genomes of three BM and three ASC donors allowed us to determine the corresponding haplogroup, as well as non-haplogroup variations. The latter were essentially common variants located in the D-loop region of mtDNA and their number or status was not observed to change during PP or expansion under hypoxia. One exception was the m.521A>G variation, which was not found in specialized databases, thus representing, to the best of our knowledge, a novel homoplasmic polymorphism. Prolonged passaging led to an increase of mtDNA content (B), intracellular ATP (iATP) (C), and membrane potential ($\Delta\psi_m$) (D), whereas expansion under hypoxia led to a decrease of more than twofold in the mtDNA content and iATP of BMSCs. *$p<0.05$, **$p<0.01$.

repeat copy number to single gene copy number (*T/S*) ratio was calculated by means of two independent amplification reactions: the telomere reaction, which proceeded for 1 cycle at 95 °C for 10 min, followed by 20 cycles at 95 °C for 5 s, 56 °C for 10 s, and 72 °C for 1 min, and the single gene reaction (*GAPDH or ACTB*) which was identical to one described above. Primer sequences are indicated in Supplementary Table 1. The *T/S* ratio for each sample was computed by subtracting the average *GAPDH* (or *ACTB*) C_T value from the average telomere C_T.

Mutational analysis of the entire mitochondrial genome

For the detection of mtDNA mutations we PCR-amplified a set of 19 overlapping fragments spanning the entire mitochondrial genome (Supplementary Table 1). PCR was performed in a 50 μl reaction volume containing 300 ng total DNA, 0.5 μM of each primer, 2.5 mM $MgCl_2$, 500 μM of each DNTP and 2.5 U of AmpliTaq Gold DNA polymerase. The PCR program consisted of an initial denaturation step of 7 min at 94 °C followed by 38 cycles of 30 s at 94 °C, 45 s at 55 °C and 1 min at 72 °C, and a final extension step of 10 min at 72 °C. After gel purification using a QIAquick gel extraction kit (Qiagen, Valencia, CA), the PCR products were sequenced and subsequently compared with the revised Cambridge Reference Sequence (rCRS, accession number NC_012920) using BLAST2Seq (www.ncbi.nlm.nih.gov/blast/bl2seq/wblast2.cgi) in order to detect polymorphisms and mutations. The former analysis was repeated in two independent PCR and sequencing reactions for both forward and reverse strands. Haplogroup-associated variants of each mtDNA contig were subsequently identified by using PhyloTree (van Oven and Kayser, 2009) (http://www.phylotree.org), and its most recent web-based application Haplogrep (http://haplogrep.uibk.ac.at/) (Kloss-Brandstatter et al., 2011).

Analysis of relative amount of mtDNA content

Total cellular DNA was isolated using the QIAamp DNA Mini Kit (Qiagen) and concentrations were spectrophotometrically determined. The content of mtDNA relative to nuclear DNA was determined by co-amplifying a 151-bp mt *ND5* fragment and a nuclear fragment from the *GAPDH* or *ACTB* genes using real time PCR. The program used was identical to that described above for gene expression analysis. Primers used are indicated in Supplementary Table 1. The ratio of mtDNA to genomic DNA was calculated with $\Delta C_T = C_T$ (*ND5*) $- C_T$ (*GAPDH* or *ACTB*). Fold difference in mtDNA content was given by $2^{-\Delta\Delta C_T}$, where $\Delta\Delta C_T = \Delta C_T$ (test group) $- \Delta C_T$ (control).

Measurement of ATP content

Intracellular ATP (iATP) content was determined by using the ATP determination kit (Invitrogen) according to manufacturer's instructions. This kit allows the determination of very low concentrations of ATP through the light-emitting oxidation of D-luciferin by luciferase. Briefly, cells were re-suspended in distilled water at a concentration of 10^6 ml^{-1}, boiled for 2 min and centrifuged (5 min, 12,000 *g*) to eliminate DNA and other cell debris. Samples were taken from the supernatant and bioluminescence was monitored at 560 nm on a multi-well bioluminescence/fluorescence plate reader (Cary Eclipse, Varian). Twenty reads were performed per well/sample and each sample was analyzed at least in triplicate.

Flow cytometric analysis of mitochondrial membrane potential ($\Delta\psi_m$)

Mitochondrial membrane potential ($\Delta\psi_m$) was evaluated by using the MitoProbe JC-1 assay kit (Molecular Probes, Eugene, OR) according to the manufacturer's instructions. Briefly, cells were detached from culture flasks, washed, and resuspended in PBS at approximately 10^6cells/ml. Cells were then incubated with the $\Delta\psi_m$-dependent cationic dye JC-1 (5,5′ 6,6′-tetrachloro-1,1′ 3,3′ tetraethylbenzimidazolcarbocyanine iodide) (2 μM final concentration) at 37 °C for 15–30 min in the dark. Uncoupling with the protonophore carbonyl cyanide 3-chlorophenylhydrazone (CCCP, final concentration 50 μM) for 30 min at 37 °C was also used as positive control. Mitochondria with elevated $\Delta\psi_m$ concentrate JC-1 into aggregates showing red fluorescence whereas mitochondria with low $\Delta\psi_m$ cannot concentrate JC-1 and show green fluorescence. Sample analysis was performed using the FACSCalibur equipment. JC-1 monomers were detected in FL1 (530/30 nm bandpass filter) while JC-1 aggregates were detected in FL2 (585/42 nm bandpass filter). At least 10,000 events were analyzed in each run and the FL2/FL1 ratio was calculated in order to reflect changes in $\Delta\psi_m$.

Statistical analysis

Data are presented as mean ± standard error of the mean (SEM) of at least three independent experiments. Comparisons were performed using a two-tail unpaired t-test or a one sample t-test (real time PCR).

Results

Morphology of SCs, immunophenotyping and *in vitro* differentiation

Morphological changes took place during the course of long-term *ex vivo* expansion of SCs. At lower passages (P1–P5), BMSCs presented a typical homogeneous fibroblast-like shape (Fig. 1A), whereas at later stages (>P10), cells acquired an enlarged, irregular and flattened shape, with inclusions and debris visible in the medium and supernatant (Fig. 1A). No differences were noticed in the morphology of BMSCs and ASCs expanded under hypoxia and normoxia (Fig. 1A, Supplementary Fig. 1A). To better evaluate the cell structural changes, we performed a morphometric analysis using the ImageJ software, in order to compute the spreading area and maximum Feret's diameter (longest distance between any two points along the cell boundary). Both parameters were found to be roughly similar between the two cell sources, and although considerably increased under PP in normoxia, they did not appear to be significantly affected in cells expanded under hypoxia (<21 days of exposure) (Fig. 1B). The average

values for cell spreading area and Feret's diameter at earlier passages were respectively 444 μm^2 and 58.5 μm. A mean fold increase of 6.5 and 2.6 was observed in the latter parameters between early and late passage cells, respectively (Fig. 1B). The number of population doublings did not change significantly between BMSCs and ASCs when these were cultured under normoxia or hypoxia for a period of 14 days, or when expanded for ten passages under normoxia (Fig. 1B).

For immunophenotypic analyses we evaluated a panel of five surface markers (Dominici et al., 2006). As expected, all SCs were positive for CD73, CD90 and CD105, and negative for CD80 and (HLA)-DR (the large majority above 99%) (Fig. 1C, BMSCs are shown as example). Similarly to what has been described by others (Bernardo et al., 2007; Dos Santos et al., 2010), no significant differences for expression of these surface markers were verified between BMSCs and ASCs expanded for a low number of passages under hypoxia and normoxia, or prolonged passaging (PP) (compare Fig. 1C with Supplementary Fig. 1C).

We have also confirmed the potential of these cells to differentiate along the adipogenic and osteogenic lineages. Oil Red O was used to stain intracellular lipid vesicles (Fig. 1D, left, BMSCs are shown as example), while alkaline phosphatase and von Kossa staining were used to identify osteogenic progenitors and calcium deposits (Fig. 1D, right, BMSCs are shown as example). Similar results were obtained for ASCs (Supplementary Fig. 1B).

Effect of hypoxia and prolonged passaging on the expression of DNA repair genes, *p53* and *c-MYC*

Since some studies have implicated hypoxia as a promoter of "stemness" and cell proliferation, we decided to investigate its effect as well as that of prolonged passaging (PP), on the expression of genes involved in HR (*RAD51*, *BRCA1*), NHEJ (*Ku80*), and MMR (*MLH1*) pathways. Low passage (P1–P3) human BMSCs and ASCs were exposed to normoxic (20% O_2) or hypoxic (2% O_2) conditions for a period of time ranging from 6 h to 21 days. After this 3-week period, normoxic cells were allowed to expand for a total of 10–20 passages (PP), while hypoxic cells were submitted to a reoxygenation period of 48 h (AR, after reoxygenation). We considered this period of reoxygenation to be long enough to allow the stabilization of gene expression profiles (if that being the case), but yet short enough to still allow evaluation of plating effects (see below).

In the first 21 days under normoxia, the expression levels of the four genes did not differ significantly from that of the control for both cell sources. (Figs. 2A and B, left). However, a surprising and rather pronounced (3- to 5-fold) increase in gene expression was observed mainly within the first 24 h upon plating for the two HR genes and for both cell sources, regardless of the O_2 tension studied (Figs. 2A and B (right), with exception for *BRCA1* in hypoxic BMSCs). Since *BRCA1* was recently implicated in the adhesion, spreading, and motility of breast cancer cells by interaction with F-actin and the ezrin/radixin/moesin complex (Coene et al., 2011), it thus seems plausible that this gene together with *RAD51*, may also play an important role in the adhesion of SCs to culture-treated plastic. Prolonged passaging in normoxia led to a significant down-regulation of *Ku80* and *BRCA1* in BMSCs, and *RAD51* and *BRCA1* in ASCs.

Under hypoxia, we observed a down-regulation of *MLH1* and *BRCA1* as soon as 6 h, but a more generalized repression of the four genes was only visible after 21 days. Moreover, changes in the expression of DNA repair genes, seemed to generally occur more slowly for ASCs than for BMSCs (compare Figs. 2A and B, right). After a 48-h period of reoxygenation, cells previously exposed to hypoxia had expression levels close to those of time 0, with the exception of *RAD51* whose over-expression was still around 4–5-fold (Figs. 2A and B, right). The latter is probably an effect reminiscent of cell passaging, which points to a delayed recovery of *RAD51* basal levels of expression.

We also evaluated the impact of hypoxia and PP on the expression of the tumor suppressor gene *p53* and the *c-MYC* proto-oncogene. Despite their well-known involvement in a plethora of biological processes that include cell-cycle progression, DNA replication, apoptosis, and angiogenesis, studies focusing on the expression levels of *p53* and *c-MYC* during *in vitro* expansion of stem cells are rather limited and have generated conflicting results. In our work we found that for both types of cells the responses of *p53* and *c-MYC* to hypoxia and prolonged passaging are similar. Upon long-term cultivation involving consecutive passages (>P10), for both BMSCs and ASCs, these genes were down-regulated (Figs. 2C and D), as previously reported by other authors (Kim et al., 2009; Efimenko et al., 2011).

Regarding the effect of hypoxia, it was previously demonstrated that it down-regulates *p53* protein levels when uncoupled from acidosis, whereas the opposite effect is seen in the presence of hypoxia-induced medium acidification (Schmaltz et al., 1998; Pan et al., 2004). In our case, the buffering capacity of the medium will in principle only allow small pH variations, which is in line with the observed *p53* repression (Figs. 2C and D). Regarding the proliferation-promoting transcription factor *c-MYC*, we have observed no effect at the transcriptional level under hypoxic conditions (Fig. 2D), in agreement with other results in the literature (reviewed by Huang, 2008). Nonetheless, severe or prolonged hypoxia is known to result in *c-MYC* degradation and its displacement from the promoter regions of MMR genes (Bindra and Glazer, 2007a). Similar gene expression data were obtained when using the beta-actin (*ACTB*) housekeeping gene instead of *GAPDH* (see Supplementary Fig. 2).

Hypoxia promotes microsatellite instability and maintains telomere length

Since down-regulation of DNA repair genes is known to induce genomic instability (Vaish, 2007; Rodriguez-Jimenez et al., 2008), we further examined the status of several microsatellite sequences present in the genomic DNA of both cell sources. The markers chosen for this analysis were TP53Alu, RB, and those belonging to the Bethesda panel (BAT25, BAT26, D5S346, D17S250, and D2S123). From day 14 onwards, we observed fragments absent in the dinucleotide markers D17S250 and D2S123 of both BMSCs and ASCs cultured under hypoxia, whereas the same instabilities and changes in D5S346 were only seen after PP for "normoxic" cells (Fig. 3A). Since MSI was found to be present in only one or two markers, it should be respectively classified as stable (MSI-S) or low frequency (MSI-L).

We also found that cells expanded under hypoxia for 14 days were able to maintain telomere length, while the latter decreased over time under normoxia, consistent with prior reports (Izadpanah et al., 2008) (Fig. 3B and Supplementary Fig. 2B). Also, no statistically significant differences were seen between BMSCs and ASCs (Fig. 3B). Previous evidence has shown that human SCs are typically telomerase-low/negative (Zimmermann et al., 2003), although contrasting results have been reported (Pittenger et al., 1999). More recently, Tsai et al. (2011) have shown that human BMSCs expanded by up to 100 population doublings under hypoxic conditions (1% O_2), had greater telomerase activity and telomere length than cells expanded under normoxia (i.e. 20%). Instead of an ectopic expression of the human telomerase gene, the authors exploit the natural ability of SCs to survive under hypoxic conditions in order to increase their lifespan. Our results are in line with these data, and extend such conclusions to human ASCs at least for a two-week period.

Effect of hypoxia and prolonged passaging on mitochondrial performance

The evaluation of mitochondrial function as a quality control procedure during *ex vivo* expansion of stem cells, has gained increasing interest in the recent years. Nevertheless, some aspects remain poorly explored, such as a thorough search for genetic aberrations in mtDNA. The results obtained in this work support the concept of a relatively stable mitochondrial genome, both in terms of small indels as well as larger aberrations. The majority of mutations found were haplogroup-specific or occurred at highly polymorphic repeat tracts, and their load did not change under hypoxia or after PP (Fig. 4A). One such example is the mononucleotide C tract ($C_{6-10}TC_6$) commonly termed D310, which is located within the displacement loop (D-loop) region. Mutations found within the D310 region were observed in all samples with exception of those from donor 2, and consisted in 1 or 2-bp C insertions (thus lying within the polymorphic length range of 6 C–10 C (Legras et al., 2008)) (Fig. 4A). The mutation m.523_524delAC found in BMSCs from donor 2 is relatively frequent and arises from slippage events occurring within a short microsatellite of 5 tandem AC repeats. Both the m.15626C>T synonymous transition located in the cytochrome b gene and m.16271T>C located in the D-loop have been previously identified (Ingman and Gyllensten, 2006; www.mitomap.org, 2011). Yet, a thorough search in the literature as well as in specialized databases (Ingman and Gyllensten, 2006; www.mitomap.org, 2011) led us to conclude that m.521A>G is most probably, a novel homoplasmic polymorphism. Another variant found in some of our samples was 16519T>C (Fig. 4A), which has been shown to be related to an increased risk of development of several types of carcinomas, or to be in linkage disequilibrium with functional variants that increase that risk (Bai et al., 2007; Peng et al., 2011).

Since some of the latter mutations map within the non-coding D-loop region involved in the regulation of replication and transcription, we hypothesized that changes in copy number could occur. In our studies with SCs, we did not find evidence of functional impairment of mitochondrial activity as a result of the presence of these mutations. In particular, we did not find significant differences in the mitochondrial content of the several donors (data not shown), suggesting that none of these mutations is *per se* the causative agent of any detrimental effect.

We further evaluated the effect of hypoxia and PP on other performance parameters such as the number of mitochondrial genomes, iATP, and membrane potential ($\Delta\psi_m$). We observed that all of the latter parameters roughly increased 1.8-fold after prolonged passaging for both cell sources (Figs. 4B–D). These changes are characteristic of a more mature state associated with differentiation or senescence (Prigione et al., 2010; Rehman, 2010).

After 21 days in hypoxia, the number of mtDNA genomes decreased more than half in BMSCs, whereas no significant difference was seen in ASCs (Fig. 4B and Supplementary Fig. 2C). These results were found to correlate with variations in iATP levels for both types of cells (Fig. 4C). Taking into consideration the role of *p53* in maintaining mtDNA oxidative phosphorylation and copy number (Lebedeva et al., 2009), its hypoxia-mediated down-regulation likely contributed to the observed decrease in iATP content and number of mitochondrial genomes. Moreover, the decrease in mtDNA content and the previously observed down-regulation of *RAD51* under hypoxia are two events that apparently cannot be dissociated. The mtDNA was recently shown to be a substrate for *RAD51*, in a pathway that possibly facilitates the completion of mtDNA replication in the presence of DNA lesions (Sage et al., 2010). Older passage cells also have an increased amount of ROS (as shown by changes in $\Delta\psi_m$) (Fig. 4D) and are more exposed to oxidative damage, a fact that may jeopardize their potential clinical use.

Discussion

In this work we have *in vitro* expanded BMSCs and ASCs under distinct oxygen tensions and PP, to specifically evaluate and compare their DNA repair machineries as well as effects on genomic stability and mitochondrial performance. First, our gene expression analysis suggests a gradual decline of DNA repair capacity over time, which may lead to a concerted decrease in stem cell function, emergence of genomic instability, and activation of apoptosis signaling pathways. Previous work has shown that the two HR genes *BRCA1* and *RAD51* are co-repressed under hypoxia through binding of E2F4/p130 complexes to their upstream promoters (Bindra et al., 2005; Bindra and Glazer, 2007b). In the case of the MMR gene *MLH1*, its transcriptional down-regulation under hypoxia has been shown to be associated with deacetylation and trimethylation of histone H3 on lysine 9, thus impairing binding of the SP1 transcriptional factor at the corresponding promoter region (Rodriguez-Jimenez et al., 2008). Regarding the expression of the NHEJ gene *Ku80*, conflicting results obtained using several cancer cell lines are reported in the literature. Meng et al. (2005) showed repression of several NHEJ gene family members following chronic hypoxia (72 h at 0.2% O_2). In another study, no change in *Ku80* expression was detected after 48 h at 0.01% O_2 (Bindra et al., 2005). Concerning the tumor supressor *p53* and the proto-oncogene *c-MYC*, they were found to be down-regulated after PP. The fact that *p53* mRNA levels may decrease or remain unaltered after PP is not necessarily at odds with its role in activating

senescence, since in some cases, up-regulation is only observed at the protein level (Izadpanah et al., 2008). Another study presents contradicting data, in the sense that it refers to the absence of significant changes in *p53* at both mRNA and protein levels after prolonged *in vitro* propagation of human SCs (Noh et al., 2010). These discrepancies may in part be due to different experimental conditions (*e.g.* culture medium), or to the use of heterogeneous cell populations that are more or less prone to enter a senescent stage. An example found in BMSCs is the link between donor age and increasing *p53* activity (Zhou et al., 2008), which supports the view that *in vivo* aging directly affects the proliferative and differentiative potential of cells *in vitro*. In the case of *c-MYC*, its expression levels have been reported to decrease during the stage of pre-senescence, increasing again as cells move towards a senescent, post-senescent or eventually to a transformed state (Rubio et al., 2008). Since all BMSCs and ASCs analyzed in this study showed evidence of entering a pre-senescence/senescence phase between P10 and P20 (in agreement with data from other studies (Bernardo et al., 2007)), the *c-MYC* down-regulation observed in these cells comes as no surprise.

We also show that down-regulation of DNA repair genes under hypoxia favoured the onset of MSI, particularly within D5S346, D17S250 and D2S123. These findings are consistent with those of several groups who have reported preferential instability in these *loci* in a wide range of MSI-L cancer cell lines (Murphy et al., 2006; Deschoolmeester et al., 2008). This bias has led to the supposition that MSI-L and MSI-H are distinct entities, which seem to arise from distinct biological processes (Murphy et al., 2006). Our MSI analysis supports this theory and further extends it to human SCs, suggesting that the onset of the MSI-L phenomenon might follow a common pathway. Others have found that lowering the O_2 percentage to 1% apparently results in an earlier onset and increase of MSI in neural stem cells and SCs, both using the Bethesda panel, as well as in other markers (Rodriguez-Jimenez et al., 2008). This fact is suggestive of an even more pronounced repression of the MMR system, and an indicator that excessively low O_2 tensions should be avoided, as they might be detrimental for genetic stability.

Currently, there is limited information on the stability of the mitochondrial genome during expansion of adult cells. A very limited number of studies have reported the detection of mutations in the mtDNA of human colonic crypt stem cells as well as in adult and embryonic primate stem cells (Taylor et al., 2003; Gibson et al., 2006). More recently, it has been suggested that stem cells may have an inherent mechanism to efficiently repair most mtDNA lesions, or they are simply not subjected to enough oxidative damage in their niche (Alison et al., 2010). In this context, one important aspect to consider is whether this scenario could be changed during *ex vivo* expansion. In this work, we recurrently found mutations occurring within the D-loop region D310. The latter has been regarded as a mutational hotspot in primary tumors, and has been described as extremely sensitive to oxidative damage and electrophilic attack (Sanchez-Cespedes et al., 2001; Peng et al., 2011). Yet, the findings that D310 mutations are also present in non-cancerous cells (albeit at a lower frequency), and that alterations are typically confined to the polymorphic length range, ultimately suggest that abnormalities in this region may be concurrent, but not causative agents of a cancerous state (Legras et al., 2008; Chatterjee et al., 2011). Curiously, an association can be established between variations in the D310 region, and the presence of a family of hot-spot motifs based around the degenerate 13-mer CCNCCNTNNCCNC. The latter has been implicated in recruiting meiotic crossover events in the human genome, as well as in promoting the mitochondrial common deletion (Myers et al., 2008). On the basis of our observation, that the D310 region matches the degenerate consensus, we hypothesize that the presence of the full 13-mer motif (or internal sub-motifs) might facilitate the occurrence of slippage events at this locus, thus enhancing the mutation rate.

Two aspects of this work merit some discussion. First, we were unable to analyze BMSCs from young donors. Nevertheless, it has been shown previously that similar down-regulation of DNA repair genes and onset of MSI under hypoxia occurs in samples from donors as young as 19 years old (Rodriguez-Jimenez et al., 2008). Secondly, one important caveat with our procedure is that hypoxic cells were passaged under normoxic conditions. This limitation is also shared with the majority of published studies that deal with low oxygen tensions. In this sense, we must recognize the need to further clarify the real impact of transiently handling hypoxia expanded cells under non-hypoxic conditions, and if this has somehow biased the conclusions of the many existing publications. Although dedicated equipment is commercially available for this purpose, its high cost has greatly limited a wider application.

One interesting detail unveiled by our data concerns the response of ASCs to hypoxic environments. Although studies focusing on the role of hypoxia on human ASCs are not abundant, these point out that low oxygen tensions do not seem to maintain stem cell characteristics or enhance proliferation in a similar fashion to what has been described for human BMSCs (Ma et al., 2009). Our results, both in terms of gene expression and mitochondrial response to hypoxia, collectively point to a similar conclusion: ASCs react to hypoxic environment more slowly than BMSCs. The reasons behind this behaviour are still unclear, but it is possible that the different characteristics of each cell niche (*e.g.* degree of vascularization, oxygen tension, cell-cell interactions), determine distinct sensitivities to hypoxia *ex vivo*. In this sense, it becomes important, from the bioengineering point of view, to clarify in more detail if the use of hypoxia during SC expansion (particularly ASC), brings any clear benefit in the typical time frames used to achieve clinically relevant cell numbers.

Conclusions

The results of this study are significant for a deeper understanding of the cellular changes that take place during *ex vivo* expansion of BMSCs and ASCs, and appear to concur with current knowledge on the use of hypoxic environments and the occurrence of replicative senescence. Relevant standardized quality controls able to characterize the myriad of changes that SCs face during culture are currently lacking, and a concerted effort is needed by both academic and clinical teams to elaborate valid guidelines. Our study suggests the adoption of procedures such as the evaluation of the status of the DNA repair machinery, analysis of a representative panel of MSI markers, and analysis of mitochondrial performance in quality control panels of culture expanded SC products. Additional

information will be needed before SCs reach the status of a fully developed, off-the-shelf therapeutic product.

Supplementary data to this article can be found online at http://dx.doi.org/10.1016/j.scr.2012.07.001.

Acknowledgments

The authors acknowledge Francisco dos Santos (IST) for providing part of the immunophenotyping data. This work was supported by Fundação para a Ciência e a Tecnologia (FCT) through the MIT-Portugal Program, Bioengineering Focus Area and Project PTDC/EQU-EQU/114231/2009. PHO acknowledges FCT for the Post-Doctoral Grant BPD/64652/2009. JSB acknowledges FCT for the Doctoral Grant BD/70948/2010.

References

Alison, M.R., McDonald, S.A., Lin, W.R., Wright, N.A., 2010. Protection of mitochondrial genome integrity: a new stem cell property? Hepatology 51, 354.

Bai, R.K., Leal, S.M., Covarrubias, D., Liu, A., Wong, L.J., 2007. Mitochondrial genetic background modifies breast cancer risk. Cancer Res. 67, 4687–4694.

Basciano, L., Nemos, C., Foliguet, B., de Isla, N., de Carvalho, M., Tran, N., Dalloul, A., 2011. Long term culture of mesenchymal stem cells in hypoxia promotes a genetic program maintaining their undifferentiated and multipotent status. BMC Cell Biol. 12, 12.

Bernardo, M.E., Zaffaroni, N., Novara, F., Cometa, A.M., Avanzini, M.A., Moretta, A., Montagna, D., Maccario, R., Villa, R., Daidone, M.G., Zuffardi, O., Locatelli, F., 2007. Human bone marrow derived mesenchymal stem cells do not undergo transformation after long-term *in vitro* culture and do not exhibit telomere maintenance mechanisms. Cancer Res. 67, 9142–9149.

Bindra, R.S., Glazer, P.M., 2007a. Co-repression of mismatch repair gene expression by hypoxia in cancer cells: role of the Myc/Max network. Cancer Lett. 252, 93–103.

Bindra, R.S., Glazer, P.M., 2007b. Repression of RAD51 gene expression by E2F4/p130 complexes in hypoxia. Oncogene 26, 2048–2057.

Bindra, R.S., Gibson, S.L., Meng, A., Westermark, U., Jasin, M., Pierce, A.J., Bristow, R.G., Classon, M.K., Glazer, P.M., 2005. Hypoxia-induced down-regulation of BRCA1 expression by E2Fs. Cancer Res. 65, 11597–11604.

Bindra, R.S., Crosby, M.E., Glazer, P.M., 2007. Regulation of DNA repair in hypoxic cancer cells. Cancer Metastasis Rev. 26, 249–260.

Bonab, M.M., Alimoghaddam, K., Talebian, F., Ghaffari, S.H., Ghavamzadeh, A., Nikbin, B., 2006. Aging of mesenchymal stem cell *in vitro*. BMC Cell Biol. 7, 14.

Caplan, A.I., 2007. Adult mesenchymal stem cells for tissue engineering versus regenerative medicine. J. Cell. Physiol. 213, 341–347.

Cawthon, R.M., 2002. Telomere measurement by quantitative PCR. Nucleic Acids Res. 30, e47.

Chatterjee, A., Dasgupta, S., Sidransky, D., 2011. Mitochondrial subversion in cancer. Cancer Prev. Res. (Phila.) 4, 638–654.

Chen, S.L., Fang, W.W., Ye, F., Liu, Y.H., Qian, J., Shan, S.J., Zhang, J.J., Chunhua, R.Z., Liao, L.M., Lin, S., Sun, J.P., 2004. Effect on left ventricular function of intracoronary transplantation of autologous bone marrow mesenchymal stem cell in patients with acute myocardial infarction. Am. J. Cardiol. 94, 92–95.

Coene, E.D., Gadelha, C., White, N., Malhas, A., Thomas, B., Shaw, M., Vaux, D.J., 2011. A novel role for BRCA1 in regulating breast cancer cell spreading and motility. J. Cell Biol. 192, 497–512.

Deschoolmeester, V., Baay, M., Wuyts, W., Van Marck, E., Van Damme, N., Vermeulen, P., Lukaszuk, K., Lardon, F., Vermorken, J.B., 2008. Detection of microsatellite instability in colorectal cancer using an alternative multiplex assay of quasi-monomorphic mononucleotide markers. J. Mol. Diagn. 10, 154–159.

Dietmaier, W., Wallinger, S., Bocker, T., Kullmann, F., Fishel, R., Ruschoff, J., 1997. Diagnostic microsatellite instability: definition and correlation with mismatch repair protein expression. Cancer Res. 57, 4749–4756.

Dominici, M., Le Blanc, K., Mueller, I., Slaper-Cortenbach, I., Marini, F., Krause, D., Deans, R., Keating, A., Prockop, D., Horwitz, E., 2006. Minimal criteria for defining multipotent mesenchymal stromal cells. The International Society for Cellular Therapy position statement. Cytotherapy 8, 315–317.

Dos Santos, F., Andrade, P.Z., Boura, J.S., Abecasis, M.M., da Silva, C.L., Cabral, J.M., 2010. *Ex vivo* expansion of human mesenchymal stem cells: a more effective cell proliferation kinetics and metabolism under hypoxia. J. Cell. Physiol. 223, 27–35.

Efimenko, A., Starostina, E., Kalinina, N., Stolzing, A., 2011. Angiogenic properties of aged adipose derived mesenchymal stem cells after hypoxic conditioning. J. Transl. Med. 9, 10.

Eibes, G., dos Santos, F., Andrade, P.Z., Boura, J.S., Abecasis, M.M., da Silva, C.L., Cabral, J.M., 2010. Maximizing the *ex vivo* expansion of human mesenchymal stem cells using a microcarrier-based stirred culture system. J. Biotechnol. 146, 194–197.

Gibson, T.C., Pei, Y., Quebedeaux, T.M., Brenner, C.A., 2006. Mitochondrial DNA deletions in primate embryonic and adult stem cells. Reprod. Biomed. Online 12, 101–106.

Gimble, J., Guilak, F., 2003. Adipose-derived adult stem cells: isolation, characterization, and differentiation potential. Cytotherapy 5, 362–369.

Horwitz, E.M., Prockop, D.J., Gordon, P.L., Koo, W.W., Fitzpatrick, L.A., Neel, M.D., McCarville, M.E., Orchard, P.J., Pyeritz, R.E., Brenner, M.K., 2001. Clinical responses to bone marrow transplantation in children with severe osteogenesis imperfecta. Blood 97, 1227–1231.

Huang, L.E., 2008. Carrot and stick: HIF-alpha engages c-Myc in hypoxic adaptation. Cell Death Differ. 15, 672–677.

Ingman, M., Gyllensten, U., 2006. mtDB: Human Mitochondrial Genome Database, a resource for population genetics and medical sciences. Nucleic Acids Res. 34, D749–D751.

Izadpanah, R., Kaushal, D., Kriedt, C., Tsien, F., Patel, B., Dufour, J., Bunnell, B.A., 2008. Long-term *in vitro* expansion alters the biology of adult mesenchymal stem cells. Cancer Res. 68, 4229–4238.

Kim, J., Kang, J.W., Park, J.H., Choi, Y., Choi, K.S., Park, K.D., Baek, D.H., Seong, S.K., Min, H.K., Kim, H.S., 2009. Biological characterization of long-term cultured human mesenchymal stem cells. Arch. Pharm. Res. 32, 117–126.

Kloss-Brandstatter, A., Pacher, D., Schonherr, S., Weissensteiner, H., Binna, R., Specht, G., Kronenberg, F., 2011. HaploGrep: a fast and reliable algorithm for automatic classification of mitochondrial DNA haplogroups. Hum. Mutat. 32, 25–32.

Lazarus, H.M., Koc, O.N., Devine, S.M., Curtin, P., Maziarz, R.T., Holland, H.K., Shpall, E.J., McCarthy, P., Atkinson, K., Cooper, B.W., Gerson, S.L., Laughlin, M.J., Loberiza Jr., F.R., Moseley, A.B., Bacigalupo, A., 2005. Cotransplantation of HLA-identical sibling culture-expanded mesenchymal stem cells and hematopoietic stem cells in hematologic malignancy patients. Biol. Blood Marrow Transplant. 11, 389–398.

Lebedeva, M.A., Eaton, J.S., Shadel, G.S., 2009. Loss of p53 causes mitochondrial DNA depletion and altered mitochondrial reactive oxygen species homeostasis. Biochim. Biophys. Acta 1787, 328–334.

Legras, A., Lievre, A., Bonaiti-Pellie, C., Cottet, V., Pariente, A., Nalet, B., Lafon, J., Faivre, J., Bonithon-Kopp, C., Goasguen, N., Penna, C., Olschwang, S., Laurent-Puig, P., 2008. Mitochondrial D310 mutations in colorectal adenomas: an early but not causative genetic event during colorectal carcinogenesis. Int. J. Cancer 122, 2242–2248.

Ma, T., Grayson, W.L., Frohlich, M., Vunjak-Novakovic, G., 2009. Hypoxia and stem cell-based engineering of mesenchymal tissues. Biotechnol. Prog. 25, 32–42.

Meng, A.X., Jalali, F., Cuddihy, A., Chan, N., Bindra, R.S., Glazer, P.M., Bristow, R.G., 2005. Hypoxia down-regulates DNA double strand break repair gene expression in prostate cancer cells. Radiother. Oncol. 76, 168–176.

Murphy, K.M., Zhang, S., Geiger, T., Hafez, M.J., Bacher, J., Berg, K.D., Eshleman, J.R., 2006. Comparison of the microsatellite instability analysis system and the Bethesda panel for the determination of microsatellite instability in colorectal cancers. J. Mol. Diagn. 8, 305–311.

Myers, S., Freeman, C., Auton, A., Donnelly, P., McVean, G., 2008. A common sequence motif associated with recombination hot spots and genome instability in humans. Nat. Genet. 40, 1124–1129.

Noh, H.B., Ahn, H.J., Lee, W.J., Kwack, K., Kwon, Y.D., 2010. The molecular signature of *in vitro* senescence in human mesenchymal stem cells. Genes & Genomics 32, 87–93.

Pan, Y., Oprysko, P.R., Asham, A.M., Koch, C.J., Simon, M.C., 2004. p53 cannot be induced by hypoxia alone but responds to the hypoxic microenvironment. Oncogene 23, 4975–4983.

Peng, Z., Xie, C., Wan, Q., Zhang, L., Li, W., Wu, S., 2011. Sequence variations of mitochondrial DNA D-loop region are associated with familial nasopharyngeal carcinoma. Mitochondrion 11, 327–333.

Pittenger, M.F., Mackay, A.M., Beck, S.C., Jaiswal, R.K., Douglas, R., Mosca, J.D., Moorman, M.A., Simonetti, D.W., Craig, S., Marshak, D.R., 1999. Multilineage potential of adult human mesenchymal stem cells. Science 284, 143–147.

Prigione, A., Fauler, B., Lurz, R., Lehrach, H., Adjaye, J., 2010. The senescence-related mitochondrial/oxidative stress pathway is repressed in human induced pluripotent stem cells. Stem Cells 28, 721–733.

Rehman, J., 2010. Empowering self-renewal and differentiation: the role of mitochondria in stem cells. J. Mol. Med. 88, 981–986.

Rodriguez-Jimenez, F.J., Moreno-Manzano, V., Lucas-Dominguez, R., Sanchez-Puelles, J.M., 2008. Hypoxia causes downregulation of mismatch repair system and genomic instability in stem cells. Stem Cells 26, 2052–2062.

Rubio, D., Garcia, S., Paz, M.F., De la Cueva, T., Lopez-Fernandez, L.A., Lloyd, A.C., Garcia-Castro, J., Bernad, A., 2008. Molecular characterization of spontaneous mesenchymal stem cell transformation. PLoS One 3, e1398.

Sage, J.M., Gildemeister, O.S., Knight, K.L., 2010. Discovery of a novel function for human Rad51: maintenance of the mitochondrial genome. J. Biol. Chem. 285, 18984–18990.

Said, H.M., Hagemann, C., Stojic, J., Schoemig, B., Vince, G.H., Flentje, M., Roosen, K., Vordermark, D., 2007. GAPDH is not regulated in human glioblastoma under hypoxic conditions. BMC Mol. Biol. 8, 55.

Sanchez-Cespedes, M., Parrella, P., Nomoto, S., Cohen, D., Xiao, Y., Esteller, M., Jeronimo, C., Jordan, R.C., Nicol, T., Koch, W.M., Schoenberg, M., Mazzarelli, P., Fazio, V.M., Sidransky, D., 2001. Identification of a mononucleotide repeat as a major target for mitochondrial DNA alterations in human tumors. Cancer Res. 61, 7015–7019.

Santos, F.D., Andrade, P.Z., Abecasis, M.M., Gimble, J.M., Chase, L.G., Campbell, A.M., Boucher, S., Vemuri, M.C., Silva, C.L., Cabral, J.M., 2011. Toward a clinical-grade expansion of mesenchymal stem cells from human sources: a microcarrier-based culture system under Xeno-free conditions. Tissue Eng. Part C Methods 17, 1201–1210.

Schmaltz, C., Hardenbergh, P.H., Wells, A., Fisher, D.E., 1998. Regulation of proliferation-survival decisions during tumor cell hypoxia. Mol. Cell. Biol. 18, 2845–2854.

Sensebe, L., Bourin, P., Tarte, K., 2011. Good manufacturing practices production of mesenchymal stem/stromal cells. Hum. Gene Ther. 22, 19–26.

Strauer, B.E., Brehm, M., Zeus, T., Kostering, M., Hernandez, A., Sorg, R.V., Kogler, G., Wernet, P., 2002. Repair of infarcted myocardium by autologous intracoronary mononuclear bone marrow cell transplantation in humans. Circulation 106, 1913–1918.

Tarte, K., Gaillard, J., Lataillade, J.J., Fouillard, L., Becker, M., Mossafa, H., Tchirkov, A., Rouard, H., Henry, C., Splingard, M., Dulong, J., Monnier, D., Gourmelon, P., Gorin, N.C., Sensebe, L., 2010. Clinical-grade production of human mesenchymal stromal cells: occurrence of aneuploidy without transformation. Blood 115, 1549–1553.

Taylor, R.W., Barron, M.J., Borthwick, G.M., Gospel, A., Chinnery, P.F., Samuels, D.C., Taylor, G.A., Plusa, S.M., Needham, S.J., Greaves, L.C., Kirkwood, T.B., Turnbull, D.M., 2003. Mitochondrial DNA mutations in human colonic crypt stem cells. J. Clin. Invest. 112, 1351–1360.

Tsai, C.C., Chen, Y.J., Yew, T.L., Chen, L.L., Wang, J.Y., Chiu, C.H., Hung, S.C., 2011. Hypoxia inhibits senescence and maintains mesenchymal stem cell properties through down-regulation of E2A-p21 by HIF-TWIST. Blood 117, 459–469.

Ueyama, H., Horibe, T., Hinotsu, S., Tanaka, T., Inoue, T., Urushihara, H., Kitagawa, A., Kawakami, K., 2012. Chromosomal variability of human mesenchymal stem cells cultured under hypoxic conditions. J. Cell Mol. Med. 16, 72–82.

Vaish, M., 2007. Mismatch repair deficiencies transforming stem cells into cancer stem cells and therapeutic implications. Mol. Cancer 6, 26.

van Oven, M., Kayser, M., 2009. Updated comprehensive phylogenetic tree of global human mitochondrial DNA variation. Hum. Mutat. 30, E386–E394.

www.mitomap.org, 2011. MITOMAP: a human mitochondrial genome database.

Yeung, S.J., Pan, J., Lee, M.H., 2008. Roles of p53, MYC and HIF-1 in regulating glycolysis — the seventh hallmark of cancer. Cell Mol. Life Sci. 65, 3981–3999.

Zhou, S., Greenberger, J.S., Epperly, M.W., Goff, J.P., Adler, C., Leboff, M.S., Glowacki, J., 2008. Age-related intrinsic changes in human bone-marrow-derived mesenchymal stem cells and their differentiation to osteoblasts. Aging Cell 7, 335–343.

Zimmermann, S., Voss, M., Kaiser, S., Kapp, U., Waller, C.F., Martens, U.M., 2003. Lack of telomerase activity in human mesenchymal stem cells. Leukemia 17, 1146–1149.